

Energetics of a global ocean circulation model compared to observations

Prasad G. Thoppil,¹ James G. Richman,¹ and Patrick J. Hogan¹

Received 31 May 2011; revised 29 June 2011; accepted 1 July 2011; published 9 August 2011.

[1] The majority of the eddy kinetic energy (EKE) in the ocean is found on scales of 50 km to 500 km, encompassed by mesoscale eddies and the meanders and rings of the boundary currents. Mesoscale eddies play a critical role in the dynamics of the ocean circulation with instabilities of the strong mean currents generating eddies in the upper ocean. Interactions between eddies transfer energy from the upper ocean to the deep ocean where eddies interact with bottom topography to generate abyssal mean flows and eddies transfer momentum back to the mean currents. The kinetic energy in a global Hybrid Coordinate Ocean Circulation Model (HYCOM) is compared with long-term observations from surface drifters, geostrophic currents from satellite altimetry, subsurface floats and deep current meter moorings. HYCOM, configured at $1/12.5^\circ$ (~ 9 km, typical of the present generation of high resolution models), is deficient in EKE in both the upper and abyssal ocean (depths greater than 3000 m) by $\sim 21\%$ and $\sim 24\%$ respectively compared to surface drifting buoys and deep current meters. Increasing the model resolution to $1/25^\circ$ (~ 4.4 km) or injecting mesoscale eddies through the assimilation of surface observations in a $1/12.5^\circ$ model increases the surface and the abyssal EKE to levels consistent with the observations. In these models, the surface (abyssal) EKE is increased by 23% (51%) and 15% (46%) for the higher resolution or data-assimilative models, respectively, compared to the $1/12.5^\circ$ non-assimilative model. While data assimilation increases the EKE in both the upper and abyssal ocean, the kinetic energy of the mean flow in the upper ocean is decreased in the data-assimilative hindcast. **Citation:** Thoppil, P. G., J. G. Richman, and P. J. Hogan (2011), Energetics of a global ocean circulation model compared to observations, *Geophys. Res. Lett.*, 38, L15607, doi:10.1029/2011GL048347.

1. Introduction

[2] The eddy kinetic energy (EKE) in the upper ocean, encompassed by mesoscale eddies, meanders and rings of the boundary currents [Stammer, 1997; Ferrari and Wunsch, 2009, 2010], is generated by instabilities of the mean flow and direct wind forcing. The present eddy-resolving global ocean general circulation models (OGCMs), running at $\sim 1/10^\circ$ horizontal grid resolution, appear to underestimate EKE at the surface compared to observations, indicating that the mean circulation is not inertial enough to generate vigorous upper ocean instabilities, which in turn is responsible for the generation of meanders and eddies. Maltrud and

McClean [2005] noted problems with too weak eddy energy in the western boundary currents and relatively quiescent regions of the global $1/10^\circ$ Parallel Ocean Program OGCM when compared to sea surface height altimetry observations. The eddy energy in the upper ocean is transferred down to the abyssal ocean by nonlinear interactions from vertically-sheared baroclinic to depth-independent barotropic states [Rhines, 1979; Hurlburt and Hogan, 2008; Ferrari and Wunsch, 2009]. In the abyssal ocean, eddies interact with bottom topography to generate a strong eddy-driven mean circulation [Holland, 1978; Rhines, 1979].

[3] Adequately representing mesoscale eddies and the energy and enstrophy (mean square vorticity) cascades in ocean models is key to simulating the mean circulation with studies suggesting that horizontal resolution around $1/10^\circ$ are sufficient [Smith et al., 2000; Oschlies, 2002; Maltrud and McClean, 2005]. However, at this resolution the models significantly underestimate the EKE in the abyssal ocean (depths greater than 3000 m) [Scott et al., 2010]. The eddy-driven mean abyssal circulation, which is constrained by the topography, can steer the mean pathways of the upper-ocean currents through a dynamical process known as upper ocean - topographic coupling [Holland, 1978; Hogan and Hurlburt, 2000; Hurlburt et al., 2008]. Recent model studies suggest that a strong eddy-driven mean abyssal circulation is sufficient to obtain a realistic Gulf Stream pathway and its separation from the western boundary [Hurlburt et al., 2008]. Thus, a strong abyssal circulation plays a critical role in the maintenance of mean circulation over the entire depth of the ocean, especially in regions dominated by intrinsic instability rather than atmospheric forcing. An intriguing question then becomes; how can we achieve a realistic representation of the abyssal ocean circulation in the OGCMs?

[4] Resolution studies [Bryan et al., 2007; Smith et al., 2000; Hogan and Hurlburt, 2000; Oschlies, 2002] show that increasing the horizontal resolution for an OGCM generates a stronger mean flow and thereby additional instabilities in the upper ocean which in turn can lead to a stronger eddy-driven abyssal circulation by vertically transferring the energy downward. Here we show that increasing the horizontal resolution from $1/12.5^\circ$ to $1/25^\circ$ yielded the most realistic representation of the ocean EKE from the surface to the abyssal ocean. All of the models clearly resolve the scales of the dominant eddies, typically the Rossby radius of deformation. Barnier et al. [2006] show that improving the representation of vorticity in eddy-permitting models improves the performance and energetics of those models. Vorticity and enstrophy are dominated by smaller scales, which benefit from an increase in resolution. Alternately, one can increase the EKE in the upper ocean indirectly by injecting eddies via assimilating ocean surface observations in a $1/12.5^\circ$ model. In this case, the additional EKE is

¹Oceanography Division, Naval Research Laboratory, Stennis Space Center, Mississippi, USA.

Report Documentation Page				Form Approved OMB No. 0704-0188	
Public reporting burden for the collection of information is estimated to average 1 hour per response, including the time for reviewing instructions, searching existing data sources, gathering and maintaining the data needed, and completing and reviewing the collection of information. Send comments regarding this burden estimate or any other aspect of this collection of information, including suggestions for reducing this burden, to Washington Headquarters Services, Directorate for Information Operations and Reports, 1215 Jefferson Davis Highway, Suite 1204, Arlington VA 22202-4302. Respondents should be aware that notwithstanding any other provision of law, no person shall be subject to a penalty for failing to comply with a collection of information if it does not display a currently valid OMB control number.					
1. REPORT DATE 29 JUN 2011		2. REPORT TYPE		3. DATES COVERED 00-00-2011 to 00-00-2011	
4. TITLE AND SUBTITLE Energetics of a global ocean circulation model compared to observations				5a. CONTRACT NUMBER	
				5b. GRANT NUMBER	
				5c. PROGRAM ELEMENT NUMBER	
6. AUTHOR(S)				5d. PROJECT NUMBER	
				5e. TASK NUMBER	
				5f. WORK UNIT NUMBER	
7. PERFORMING ORGANIZATION NAME(S) AND ADDRESS(ES) Naval Research Laboratory, Oceanography Division, Stennis Space Center, MS, 39529				8. PERFORMING ORGANIZATION REPORT NUMBER	
9. SPONSORING/MONITORING AGENCY NAME(S) AND ADDRESS(ES)				10. SPONSOR/MONITOR'S ACRONYM(S)	
				11. SPONSOR/MONITOR'S REPORT NUMBER(S)	
12. DISTRIBUTION/AVAILABILITY STATEMENT Approved for public release; distribution unlimited					
13. SUPPLEMENTARY NOTES					
14. ABSTRACT					
15. SUBJECT TERMS					
16. SECURITY CLASSIFICATION OF:			17. LIMITATION OF ABSTRACT Same as Report (SAR)	18. NUMBER OF PAGES 6	19a. NAME OF RESPONSIBLE PERSON
a. REPORT unclassified	b. ABSTRACT unclassified	c. THIS PAGE unclassified			

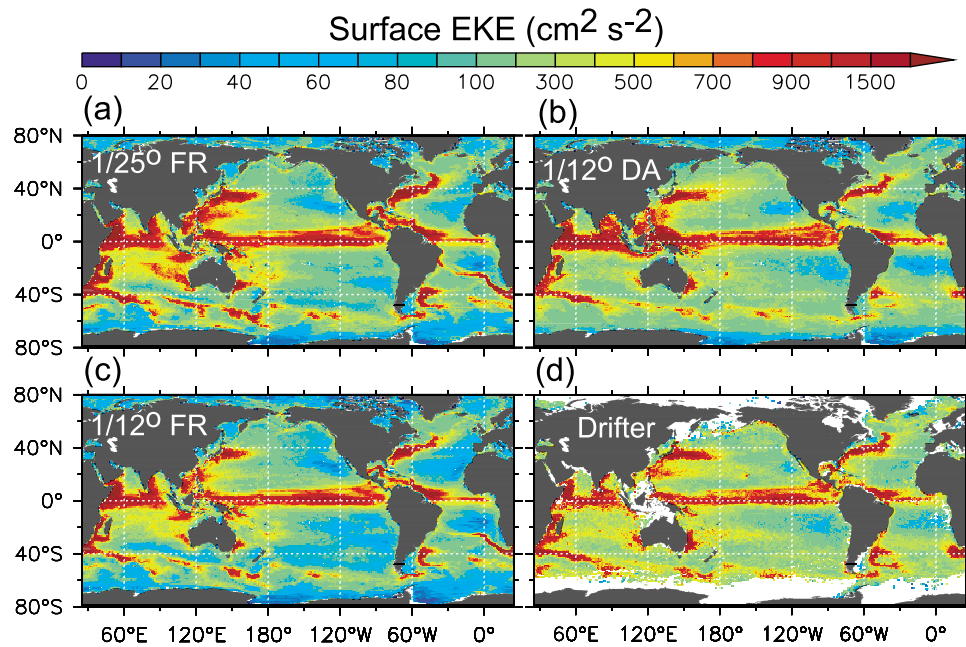


Figure 1. Surface eddy kinetic energy (EKE in $\text{cm}^2 \text{s}^{-2}$) from the three numerical experiments (a) $1/25^\circ$ FR (2005–2009), (b) $1/12.5^\circ$ DA (2008–2009), and (c) $1/12.5^\circ$ FR (2005–2009) and (d) drifter observations encompassing the period 1983–2009. The surface drift observations are binned into $1^\circ \times 1^\circ$ grids using daily values and those grid points with at least 100 observations are considered. The EKE is computed from the daily velocity fields using the equation $(\langle u'^2 \rangle + \langle v'^2 \rangle)/2$, where brackets indicate time means and primes denote deviations from the time-mean velocities, $(u', v') = (u, v) - (\langle u \rangle, \langle v \rangle)$.

generated by eddies introduced through data assimilation rather than intrinsic instability of the ocean dynamics. Our results indicate a significant increase in the abyssal ocean EKE when data assimilation is included. The major focus of attention in this paper is the comparative global ocean energetics from observations, employing four independent sets of observations representing the entire water column, and twin model experiments, only varying in horizontal resolution, horizontal eddy viscosity and data assimilation.

2. Model and Data

[5] To explore why the current generation of eddy-resolving OGCMs at $\sim 1/10^\circ$ resolution are deficient in EKE, we set-up three model experiments differing only in horizontal resolution and data assimilation. The models are a $1/12.5^\circ$ (~ 9 km at the Equator) and a $1/25^\circ$ (~ 4.4 km at the Equator) horizontal resolution non-assimilative models, denoted respectively as $1/12.5^\circ$ FR and $1/25^\circ$ FR and a $1/12.5^\circ$ with data assimilation, denoted as $1/12.5^\circ$ DA. The numerical model is the HYbrid Coordinate Ocean Model (HYCOM) [Bleck, 2002], which has 32 hybrid layers in the vertical and is forced with three-hourly, 0.5° NOGAPS atmospheric fields. The model is spun-up from rest using the GDEM3 climatology for 10 years. Thereafter, the model is forced with interannually varying NOGAPS atmospheric fields from 2003 to 2009. The analysis is performed with the last five years of the model run (2005–2009). The impact of data assimilation is examined in a $1/12.5^\circ$ model for the period 2008–2009, where observations of satellite derived sea surface height (SSH) and vertical profiles of temperature are incrementally updated using a MultiVariate Optimal Interpolation scheme [Cummings, 2005]. The SSH anomaly

lies are not directly assimilated, but converted into synthetic profiles of temperature and salinity in the upper ocean for assimilation.

[6] The modeled energetics are compared to four independent sets of observations for four different dynamical regimes representing (1) surface (2) below the wind-driven mixed layer (150 m) (3) near the permanent thermocline (1000 m) and (4) abyssal ocean. At the surface, the instabilities of the mean flow and direct wind forcing dominate the energetics while quasi-geostrophy controls the energy below the mixed-layer and in the thermocline. In the abyssal ocean the interaction of mean flow with the topography generates an eddy-driven abyssal circulation. We use surface drifter observations [Lumpkin and Pazos, 2007], satellite altimetry (150 m) [Ducet et al., 2000], ARGO floats at 1000 m [Lebedev et al., 2007], and deep current moorings [Scott et al., 2010] for model comparison to observations.

3. Results

[7] A comparison of surface EKE among the models show high levels of EKE ($>800 \text{ cm}^2 \text{s}^{-2}$) concentrated in the vicinity of the major current systems associated with the Gulf Stream and its continuation as the North Atlantic Current, the Loop Current in the Gulf of Mexico, the Brazil Current, the Kuroshio (off Japan), the equatorial current system and, in the southern hemisphere, the Antarctic Circumpolar Current (ACC), Agulhas Current (off southeast Africa), Eastern Australian Current, and Leeuwin Current near the western coast of Australia (Figure 1). The models reproduce the major circulation features observed with the drifting buoys (Figure 1d), as indicated by the high spatial correlation (~ 0.8) between the model and observed EKE (Table 1).

Table 1. Observed and Modeled Eddy and Mean Kinetic Energy^a

	Surface ^b		150 m ^c	1000 m ^d	Abyssal Ocean ^b		Abyssal Ocean ^e	
	EKE ^f (cm ² s ⁻²)	KEM (cm ² s ⁻²)	EKE ^f (cm ² s ⁻²)	EKE ^f (cm ² s ⁻²)	EKE (cm ² s ⁻²)	KEM (cm ² s ⁻²)	EKE (cm ² s ⁻²)	KEM (cm ² s ⁻²)
1/12.5° FR	343	171	121	26.4	8.37	2.81	13.27	6.84
(2005–2009)	(0.81) ^g	(0.69)	(0.64)	(0.77)			(0.71)	(0.51)
1/25° FR	423	193	181	37.9	12.61	4.44	18.28	8.54
(2005–09)	(0.82)	(0.67)	(0.70)	(0.77)			(0.80)	(0.54)
1/12.5° DA	393	160	123	33.7	12.24	3.48	14.17	6.83
(2008–09)	(0.77)	(0.67)	(0.79)	(0.71)			(0.80)	(0.33)
Observations	436	135	159	27.5			17.73	8.21

^aAbbreviations used: EKE, eddy kinetic energy; KEM, kinetic energy of mean flow computed using the equation $(\langle u^2 \rangle + \langle v^2 \rangle)/2$, where brackets denote time means; FR, non-assimilative simulation; DA, data assimilative hindcast.

^bMean over the global ocean (70°S–70°N).

^cMean over the global ocean (60°S–60°N) excluding the tropical ocean (5°S–5°N) where the assumption of geostrophy leads to potentially large errors.

^dMean over the global ocean (70°S–70°N) using 3° × 3° grid.

^eMean values obtained at the 712 current meter mooring locations.

^fDue to the unrealistic Agulhas overshooting into the south Atlantic in the simulations, the region bounded by 20°W–10°E, 40°–20°S is excluded from mean.

^gThe correlation coefficient between the model and observed kinetic energy.

However, quantitatively the global mean EKE among the models differ significantly from the drifter observations, 1/25° FR being the closest. The 1/12.5° FR model underestimates the global mean EKE by 21% relative to the drifting buoys (Table 1) implying weaker flow instabilities and fewer meanders. For the higher resolution model, the surface EKE increases by 23% from 343 cm² s⁻² in the 1/12.5° FR to 423 cm² s⁻², which is 97% of the observed EKE (436 cm² s⁻²). Since the models are forced by identical atmospheric fields, the increase in EKE with resolution arises primarily from increased baroclinic and barotropic instability of the stronger mean flow in the higher resolution model, which generates more meanders and eddies with a corresponding increase in EKE. Interestingly, the EKE in the 1/12.5° DA experiment increases by 15% to 393 cm² s⁻², which is 90% of the observed EKE, through the alteration and insertion of eddies via assimilation of surface observations. Thus, both the resolution and the data assimilation increase the overall global mean surface EKE, by 23% and 15% respectively.

[8] There are, however, obvious model-data discrepancies of the spatial distribution of EKE in the simulations. For example, a band of high EKE associated with the anticyclonic rings from the Agulhas Current (AC) at its retroflection, occurs in non-assimilative simulations, but is not observed. The model tends to shed AC rings at regular intervals which follow a wrong pathway northwestward into the South Atlantic with little dissipation. The resulting elongated band of high EKE is a known artifact of the model [and in other global models as well, e.g. Barnier *et al.*, 2006], although the exact cause remains to be determined. Exclusion of this region (20°W–10°E, 40°–20°S) from the global EKE statistics presented in Table 1 had small impact. Two other regions with significant departure from the observations are the large EKE off Java/Indonesia and the Southeast Indian Ocean (seen only in 1/25° FR). An examination of altimeter derived EKE in these regions do show similar patterns but with much lower amplitudes, suggesting inadequate coverage by the drifting buoys. The model-drifter differences in relatively quiescent regions (e.g. a bias toward lower EKE in the southeast Pacific ~30°S) can be attributed,

in part, to the atmospheric forcing. Overall the 1/25° FR model appears to be somewhat too energetic in those regions where intrinsic instability dominates the mesoscale eddies. In these highly energetic regions, the estimated drifter EKE may be underestimated due to the tendency of the drifting buoys to accumulate in regions of weak flow [Pasquero *et al.*, 2007].

[9] The increase in EKE with resolution is associated with a stronger mean circulation. Narrow bands of high kinetic energy of the mean flow (KEM >700 cm² s⁻²) are evident in the regions of large EKE with moderate spatial correlation of ~0.67 between the model energy levels and the drifter observations (Table 1). The KEM, also, increases by 13% in the higher resolution simulation, from 171 cm² s⁻² in 1/12.5° FR to 193 cm² s⁻² in 1/25° FR, indicating a stronger mean circulation with increased generation of meanders and eddies through flow instabilities. The simulated KEM, however, is systematically higher than the drifter estimates by 21% and 42% respectively. The model-observation difference may arise from two possible sources; (1) drifting buoys tend to accumulate in regions of weak flow leading to a low bias in the mean flow and (2) the analysis period for the models (2005–2009) is much shorter than the 22 years of buoy history. While data assimilation increases the surface EKE, the KEM is weaker in 1/12.5° DA compared to the other simulations. Among the models, the spatial pattern of KEM in the 1/12.5° DA depicts a better agreement with the drifter observations with a mean value of 160 cm² s⁻².

[10] Below the wind-driven mixed layer, quasi-geostrophic flow dominates the EKE, while Ekman currents add to the surface EKE. Geostrophic velocity estimates from mapped satellite altimeter SSH [Duquet *et al.*, 2000] need to be compared to the model currents below the mixed layer rather than the surface flow. At 150 m, which is below the wind-driven mixed layer, the EKE of the 1/25° FR is the highest at 181 cm² s⁻², exceeding the altimeter estimate by 14%. Both 1/12.5° FR and 1/12.5° DA have nearly the same EKE (122 cm² s⁻²), approximately 23% below the altimeter estimate (159 cm² s⁻²). The 1/12.5° models rapidly attenuate the EKE with depth which makes a quantitative comparison with the surface geostrophic velocity difficult. Among the

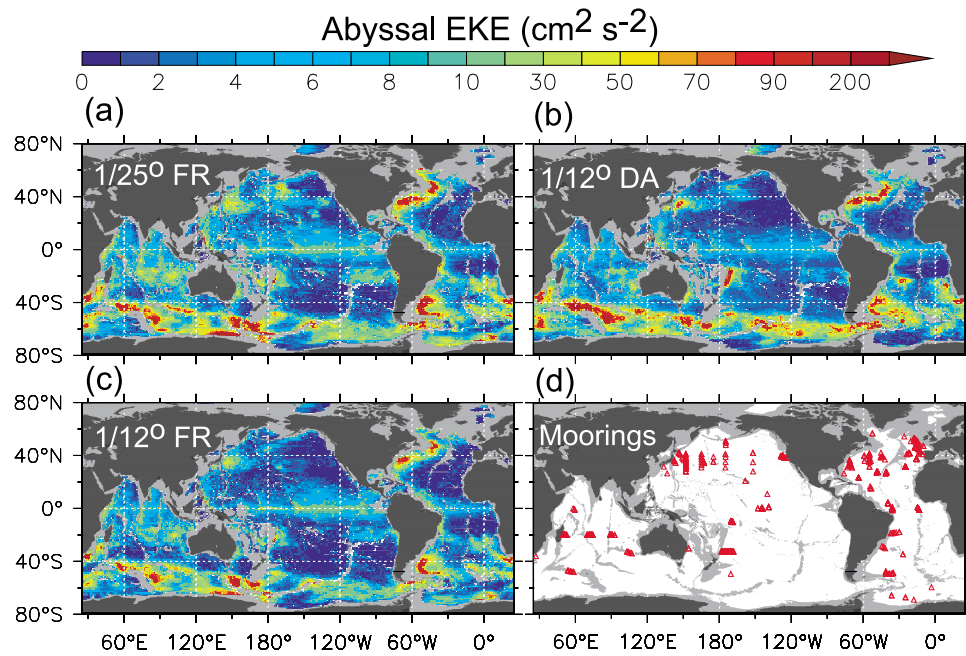


Figure 2. Abyssal ocean EKE ($\text{cm}^2 \text{s}^{-2}$) averaged below 3000 m from the three numerical experiments (a) $1/25^\circ$ FR, (b) $1/12.5^\circ$ DA, and (c) $1/12.5^\circ$ FR and (d) locations of the 712 deep current meter moorings used to validate the model kinetic energy (see *Scott et al.* [2010] for details). Moorings with a record at least 180 days are considered. Depths less than 3000 m are masked grey.

models, $1/12.5^\circ$ DA is most highly correlated with the altimeter EKE with a correlation coefficient of 0.79. It should be noted that the energy estimates from the SSH are affected by sampling artifacts. The mapped geostrophic velocity estimates will be lower than the true geostrophic velocity due to the removal of variability on times shorter than approximately 10 days and horizontal scales smaller than approximately 50 km.

[11] We use subsurface drift vectors at 1000 m from the ARGO floats [*Lebedev et al.*, 2007] to examine the EKE near the thermocline. Again, the energy estimates from the ARGO float are subjected to sampling errors. The number of ARGO floats is much smaller than the number of surface drifters. For the past 5 years, approximately 3000 ARGO floats have returned a position observation every 10 days. Thus, the sampling of the ARGO floats is coarser in space and time with a shorter history than surface drifters. The drift vectors are binned on a $3^\circ \times 3^\circ$ grid to get at least 100 observations in each grid box. Given the small sample size, the ARGO EKE estimates are expected to be biased low. At 1000 m, the higher resolution and data assimilative model EKE exceed the $1/12.5^\circ$ FR by 44% (26.4 to $37.9 \text{ cm}^2 \text{s}^{-2}$) and 28% (26.4 to $33.7 \text{ cm}^2 \text{s}^{-2}$) respectively, similar to the surface EKE (Table 1). The $1/12.5^\circ$ FR underestimates the observed EKE by 4%.

[12] Eddies in the upper ocean have a significant impact on the abyssal circulation (depths greater than 3000 m), as abyssal eddies are created via vertical transfer of eddy energy into the abyssal ocean. In the models, high abyssal ocean EKE (80 – $300 \text{ cm}^2 \text{s}^{-2}$) is located beneath the regions of high surface EKE such as western boundary currents and the ACC (Figure 2), a strong indicator of vertical transfer of EKE from the surface to the abyssal ocean. For the global

abyssal ocean, the EKE increases by 51% from $8.4 \text{ cm}^2 \text{s}^{-2}$ to $12.6 \text{ cm}^2 \text{s}^{-2}$ when the resolution is doubled (Table 1). In the $1/12.5^\circ$ DA, with additional surface eddies introduced by the assimilation of sea surface height driving a stronger eddy-driven abyssal circulation, the EKE increases by a comparable extent of 46% to $12.2 \text{ cm}^2 \text{s}^{-2}$. A comparison of model EKE with 712 moored current meter records (from a collection described by *Scott et al.* [2010]) indicates that the $1/25^\circ$ FR has the most realistic representation of abyssal ocean EKE and the $1/12.5^\circ$ FR underestimates the EKE by 24%. At these locations, the EKE increased from $13.3 \text{ cm}^2 \text{s}^{-2}$ in $1/12.5^\circ$ FR to $18.3 \text{ cm}^2 \text{s}^{-2}$ in the $1/25^\circ$ FR, comparable with the observed current meter measurements ($17.7 \text{ cm}^2 \text{s}^{-2}$, Table 1). When correlated spatially with the current meter observations, both $1/25^\circ$ FR and $1/12.5^\circ$ DA EKE have higher correlation (~ 0.8) compared to $1/12.5^\circ$ FR (0.71). For the mean global abyssal circulation, the KEM increases by 58% for $1/25^\circ$ FR and 24% with data assimilation. However, at the current meter locations the KEM increases by 25% for the higher resolution simulation, but remains virtually unchanged with data assimilation.

[13] Noting that the abyssal EKE is greatest beneath the regions of high surface EKE, we have extracted the Gulf Stream region (80°W – 30°W , 10°N – 60°N) for closer examination. The overall patterns of surface EKE in both $1/12.5^\circ$ DA and $1/25^\circ$ FR are similar to the drifter observations (Figures 3a–3d). In $1/12.5^\circ$ FR, the simulated EKE along the North Atlantic Current between 55°W and 35°W is significantly underestimated. In the abyssal ocean, it is clear from the superimposed current meter observations in Figures 3e–3g that both the higher resolution and data assimilative models have realistic EKE below the Gulf Stream. The $1/12.5^\circ$ FR EKE is too low east of 60°W , typically by a factor of

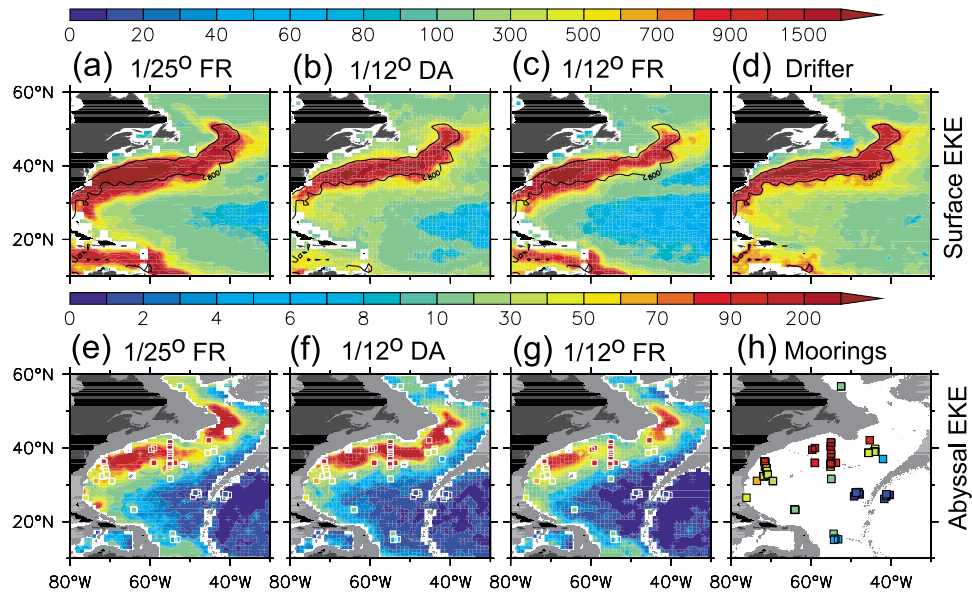


Figure 3. The EKE in the Gulf Stream region. Surface EKE ($\text{cm}^2 \text{s}^{-2}$) for the three numerical experiments (a) $1/25^\circ$ FR, (b) $1/12.5^\circ$ DA, and (c) $1/12.5^\circ$ FR with the $800 \text{ cm}^2 \text{s}^{-2}$ contour from the (d) drifter observations superimposed on the model surface EKE. Abyssal ocean EKE ($\text{cm}^2 \text{s}^{-2}$) averaged below 3000 m for the Gulf Stream region from the three numerical experiments (e) $1/25^\circ$ FR, (f) $1/12.5^\circ$ DA, and (g) $1/12.5^\circ$ FR with superimposed EKE estimates from the (h) moored current meter observations shown as color filled squares (same color shading for both models and the observations). Depths less than 3000 m are masked grey.

two and too weak farther to the west consistent with the weaker surface EKE.

4. Conclusions

[14] We compare the energetics of a global ocean general circulation model with a variety of observations from surface to the abyssal ocean. The surface and abyssal circulation of the ocean are strongly coupled through the energy cascades that vertically redistribute the energy and vorticity throughout the entire water column. The surface kinetic energy of ocean circulation is dominated by eddy kinetic energy (EKE) associated with the instabilities of the mean flow and direct wind forcing. The eddy-eddy interactions transfer energy, initially, from large scales towards the Rossby radius scale and vorticity towards small scales. At scales near the Rossby radius, energy is transferred from the upper ocean into the abyssal ocean. The abyssal eddies interact with topography to generate mean flows. The EKE in a $1/12.5^\circ$ non-assimilative model is deficient and accounts for only about 79% and 76% of the observations at the surface and at the abyssal ocean, respectively. Increasing the model resolution ($1/25^\circ$) which generates a stronger mean flow and thereby additional instabilities with a corresponding impact on the nonlinear cascades of energy or injecting eddies via assimilating ocean surface observations improves the model energetics to be consistent with independent observations from the surface to the abyssal ocean. In the models, high abyssal ocean EKE ($80\text{--}300 \text{ cm}^2 \text{s}^{-2}$) is located beneath the regions of high surface EKE such as western boundary currents and the ACC, a strong indicator of vertical transfer of EKE from the surface to the abyssal ocean. A comparison of model EKE with 712 moored current meter records indicates

that the $1/25^\circ$ FR has the most realistic representation of abyssal ocean EKE with a correlation coefficient of 0.8. An increase in the surface EKE by 23% (15%) and a corresponding 51% (46%) increase in the abyssal EKE in the $1/25^\circ$ FR ($1/12.5^\circ$ DA) model clearly demonstrates the need for better representation of upper ocean EKE as a prerequisite for strong eddy-driven abyssal circulation. Although the present generation of eddy-resolving global OGCMs at $1/10^\circ$ resolve the dominant eddy scale, our model experiments suggest resolving the nonlinear eddy interactions and associated transfer of energy significantly affects the performance of the models.

[15] **Acknowledgments.** This work was supported in part by a grant of computer time from the DOD High Performance Computing Modernization Program at the Navy DSRC. It was sponsored by the Office of Naval Research (ONR) through the NRL projects, Eddy Resolving Global Ocean Prediction Including Tides, Ageostrophic Vorticity Dynamics of the Ocean and Full Column Mixing for Numerical Ocean Models. We thank Robert Scott of the Université de Bretagne Occidentale for providing the historical current meter data and Joseph Metzger, Ole Martin Smedstad, and Luis Zamudio for making the global HYCOM simulations available.

[16] The Editor thanks two anonymous reviewers for their assistance in evaluating this paper.

References

- Barnier, B., et al. (2006), Impact of partial steps and momentum advection schemes in a global ocean circulation model at eddy-permitting resolution, *Ocean Dyn.*, **56**, 543–567, doi:10.1007/s10236-006-0082-1.
- Bleck, R. (2002), An oceanic general circulation model framed in hybrid isopycnic-Cartesian coordinates, *Ocean Modell.*, **4**, 55–88, doi:10.1016/S1463-5003(01)00012-9.
- Bryan, F. O., M. W. Hecht, and R. D. Smith (2007), Resolution convergence and sensitivity studies with North Atlantic circulation models. Part I: The western boundary current system, *Ocean Modell.*, **16**, 141–159, doi:10.1016/j.ocemod.2006.08.005.

- Cummings, J. A. (2005), Operational multivariate ocean data assimilation, *Q. J. R. Meteorol. Soc.*, **131**, 3583–3604, doi:10.1256/qj.05.105.
- Ducet, N., P.-Y. Le Traon, and G. Reverdin (2000), Global high resolution mapping of ocean circulation from TOPEX/Poseidon and ERS-1 and 2, *J. Geophys. Res.*, **105**, 19,477–19,498, doi:10.1029/2000JC900063.
- Ferrari, R., and C. Wunsch (2009), Ocean circulation kinetic energy: Reservoirs, sources and sinks, *Annu. Rev. Fluid Mech.*, **41**, 253–282, doi:10.1146/annurev.fluid.40.111406.102139.
- Ferrari, R., and C. Wunsch (2010), The distribution of eddy kinetic and potential energies in the global ocean, *Tellus, Ser. A*, **62**, 92–108.
- Hogan, P. J., and H. E. Hurlburt (2000), Impact of upper ocean–topographic coupling and isopycnal outcropping in Japan/East Sea models with $1/8^\circ$ to $1/64^\circ$ resolution, *J. Phys. Oceanogr.*, **30**, 2535–2561, doi:10.1175/1520-0485(2000)030<2535:IOUOTC>2.0.CO;2.
- Holland, W. R. (1978), The role of mesoscale eddies in the general circulation of the ocean—Numerical experiments using a wind-driven quasi-geostrophic model, *J. Phys. Oceanogr.*, **8**, 363–392, doi:10.1175/1520-0485(1978)008<0363:TROMEI>2.0.CO;2.
- Hurlburt, H. E., and P. J. Hogan (2008), The Gulf Stream pathway and the impacts of the eddy-driven abyssal circulation and the deep western boundary current, *Dyn. Atmos. Oceans*, **45**, 71–101, doi:10.1016/j.dynatmoce.2008.06.002.
- Hurlburt, H. E., E. J. Metzger, P. J. Hogan, C. E. Tilburg, and J. F. Shriver (2008), Steering of upper ocean currents and fronts by the topographically constrained abyssal circulation, *Dyn. Atmos. Oceans*, **45**, 102–134, doi:10.1016/j.dynatmoce.2008.06.003.
- Lebedev, K. V., H. Yoshinari, N. A. Maximenko, and P. W. Hacker (2007), Velocity data assessed from trajectories of Argo floats at parking level and at the sea surface, *Tech. Note 4(2)*, 16 pp., Int. Pac. Res. Cent., Honolulu, Hawaii.
- Lumpkin, R., and M. Pazos (2007), Measuring surface currents with Surface Velocity Program drifters: The instrument, its data, and some recent results, in *Lagrangian Analysis and Prediction of Coastal and Ocean Dynamics*, edited by A. Griffa et al., pp. 39–67, Cambridge Univ. Press, Cambridge, U. K.
- Maltrud, M. E., and J. L. McClean (2005), An eddy resolving global $1/10^\circ$ ocean simulation, *Ocean Modell.*, **8**, 31–54, doi:10.1016/j.ocemod.2003.12.001.
- Oschlies, A. (2002), Improved representation of upper-ocean dynamics and mixed-layer depths in a model of the North Atlantic on switching from eddy-permitting to eddy-resolving grid resolution, *J. Phys. Oceanogr.*, **32**, 2277–2298, doi:10.1175/1520-0485(2002)032<2277:IROUOD>2.0.CO;2.
- Pasquero, C., A. Bracco, A. Provenzale, and J. B. Weiss (2007), Particle motion in a sea of eddies, in *Lagrangian Analysis and Prediction of Coastal and Ocean Dynamics*, edited by A. Griffa et al., pp. 89–118, Cambridge Univ. Press, Cambridge, U. K., doi:10.1017/CBO9780511535901.005.
- Rhines, P. B. (1979), Geostrophic turbulence, *Annu. Rev. Fluid Mech.*, **11**, 401–440, doi:10.1146/annurev.fl.11.010179.002153.
- Scott, R. B., B. K. Arbic, E. P. Chassignet, A. C. Coward, M. Maltrud, W. J. Merryfield, A. Srinivasan, and A. Varghese (2010), Total kinetic energy in four global eddying ocean circulation models and over 5000 current meter records, *Ocean Modell.*, **32**, 157–169, doi:10.1016/j.ocemod.2010.01.005.
- Smith, R. D., M. Maltrud, F. O. Bryan, and M. W. Hecht (2000), Numerical simulation of the North Atlantic Ocean at $1/10^\circ$, *J. Phys. Oceanogr.*, **30**, 1532–1561, doi:10.1175/1520-0485(2000)030<1532:NSOTNA>2.0.CO;2.
- Stammer, D. (1997), Global characteristics of ocean variability estimated from regional TOPEX/Poseidon altimeter measurements, *J. Phys. Oceanogr.*, **27**, 1743–1769, doi:10.1175/1520-0485(1997)027<1743:GCOOVE>2.0.CO;2.

P. J. Hogan, J. G. Richman, and P. G. Thoppil, Oceanography Division, Naval Research Laboratory, Stennis Space Center, MS 39529, USA. (prasad.thoppil@nrlssc.navy.mil)